Preprint of: Wojnowski, T., Ordyszewska, A., Halenka, H., Anusiewicz, I., Chojnacki, J., Kaniewska-Laskowska, K., & Grubba, R. (2025). Activation of small molecules by ambiphilic NHC-stabilized phosphinoborenium cation: formation of boreniums with B–O–C, B–O–B, and B–O–P structural motifs. DALTON TRANSACTIONS, 54, 290-297. https://doi.org/10.1039/d4dt02656j

ARTICLE

Activation of small molecules by ambiphilic NHC-stabilized phosphinoborenium cation: formation of boreniums with B-O-C, B-O-B, and B-O-P structural motifs

Tomasz Wojnowski,[a] Anna Ordyszewska,[a] Hanna Halenka,[a] Iwona Anusiewicz,[b] Jarosław Chojnacki,[a] Kinga Kaniewska-Laskowska,[a] and Rafał Grubba[a]*

The reactivity of the phosphinoborenium cation supported by a 1,3,4,5-tetramethylimidazolin-2-ylidene ligand toward small molecules was explored. The phosphinoborenium cation exhibited dual Lewis acid–base properties due to the presence of the Lewis acidic boron center and the Lewis basic phosphido ligand connected by a covalent bond. The reaction of the title cation with CO_2 led to the insertion of a CO_2 molecule into the P-B bond. The obtained borenium CO_2-adduct underwent hydrolysis, forming an *N*-heterocyclic carbene stabilized diborenium dication bearing a B-O-B functionality. The activation of N_2O proceeded via the insertion of an oxygen atom into the B-P bond of the parent cation, yielding a borenium cation with a phosphinite moiety. An alternative synthetic pathway to borenium cations with a B-O-P skeleton was achieved via the activation of secondary phosphine oxides by the phosphinoborenium cation. Furthermore, borenium cations and diborenium dications with B-O-C structural motifs were obtained from the reaction of the title compound with perfluorinated *tert*-butyl alcohol and hydroquinone, respectively. The structure of the obtained borenium cations is discussed based on multinuclear NMR spectroscopy, X-ray diffraction, and density functional theory calculations.

Introduction

The study of boron chemistry has long fascinated researchers due to this element's unique properties and versatile applications. Within this field, the synthesis, reactivity, and application of boron cations—a class of electrophilic boron species—have garnered significant interest[1–3]. These cations are characterized by a positively charged boron atom bonded to two, three, or four substituents (R) or ligands (L). These species are called borinium ($[BR_2]^+$), borenium ($[(L)BR_2]^+$), and boronium $[(L)_2BR_2]^+$), respectively.

One of the key challenges associated with borenium cations, the compound of interest, is their inherent instability and high reactivity, making them difficult to isolate and study. However, recent advancements have demonstrated that *N*-heterocyclic carbenes (NHCs) can effectively stabilize borenium cations,[4] enabling detailed exploration of their reactivity and potential applications.[5] The first stabilized borenium cation $[Mes_2BIMe_2]^+$ (IMe_2 = 1,3-dimethylimidazol-2-ylidiene) was synthesized in 2009 by Matsumoto and Gabbaï in a reaction involving Mes_2BF, TMSOTf, and $[Ag(IMe_2)_2][Ag_2I_3]$.[6] Since then, a large group of borenium cations stabilized with NHCs[7–14] have been obtained because NHCs provide electronic stabilization through the donation of electron density into the vacant *p* orbital of boron. This interaction enhances the stability of the borenium cation and modifies its reactivity profile, opening avenues for novel chemical transformations such as stoichiometric and catalytic reactions (e.g., hydrosilylation, hydroboration, C-H activation).

There are a plethora of examples using borenium cations in metal-free catalytic reactions[15] that have been discovered in recent years. One of the most studied reactions is a hydrogenation reaction that can be catalyzed by borenium cations, among other catalysts, in an FLP-type reaction, as described by Stephan *et al.*[12,16]. A *meso*-ionic carbene (MIC)-borenium was also found to be an effective hydrogenation catalyst under mild conditions.[17] Another portion of borenium-catalyzed hydrogenation was investigated by Speed *et al.,* who developed a bis(amino)cyclopopenylidiene-stabilized borenium catalyst used in the hydrogenation reaction of imines.[18] In addition, chiral borenium ions were tested in an enantioselective hydrogenation[19,20].

A different type of widely studied reaction is hydroboration. NHC-stabilized borenium cations, IMe_2-BH_2-NTf_2, can produce hydroboration as well as dihydroboration reaction products in reactions with alkenes.[21] When NTf_2^- is replaced with I^-, selective monohydroboration is observed. Additionally, different types of alkenes can be used in these reactions.[22] In addition, silyl-substituted alkynes were investigated and yielded unexpected 1,1-hydroboration products.[23] Studies on hydroboration involve in addition reactions with esters.[24] Transhydroboration of terminal alkynes can be achieved by using borenium cations $[NHC(9\text{-}BBN)]^+$ (9-BBN = 9-

[a] Department of Inorganic Chemistry, Faculty of Chemistry and Advanced Materials Center, Gdańsk University of Technology, Narutowicza 11/12, 80-233 Gdańsk, Poland. E-mail: rafal.grubba@pg.edu.pl
[b] Laboratory of Quantum Chemistry, Department of Theoretical Chemistry, Faculty of Chemistry, University of Gdańsk, Wita Stwosza 63, 80-308 Gdańsk, Poland.
Electronic Supplementary Information (ESI) available: Experimental, crystallographic, spectroscopic and computational details. See DOI: 10.1039/x0xx00000x

borabicyclo(3.3.1)nonane) giving *Z*-vinylboranes.[25] Regio- and stereoselective haloboration of terminal alkynes and internal alkynes was obtained in a simple one-pot reaction of selected borenium cations $[X_2B(2\text{-DMAP})]^+$ (X = Cl, Br, Ph).[26] C-H borylation is a different powerful and versatile tool involving borenium cations that enables the direct functionalization of C-H bonds, providing access to a wide range of valuable organoboron compounds[27–29]. In addition, borenium catalysts can activate C-C bonds in reaction with cyclopropanes because of their high electrophilicity.[30]

There are also limited reports on phosphine-stabilized borenium cations, which are a relatively new group of boron cationic species. Bourissou has reported on a naphthyl-bridged B/P cation and its reactivity toward H_2 and 3-hexyne,[31] as well as showed its reactivity with $PhNH_2$, NH_3, and $HNTf_2$.[32] Kong synthesized and investigated a boron dication supported by an amido diphosphine pincer ligand and showed its reactivity in a variety of stoichiometric and catalytic reactions.[33] In addition, Stephan reported the formation of $[(C_6H_4O_2)BPtBu_2R]^+$ (R= *t*Bu, $C_6H_4(C_6H_5)$) in the reaction of catecholborane with an equivalent of selected bulky tertiary phosphine and $B(C_6F_5)_3$; however, the density functional theory (DFT) calculations suggest that it is best described as a boryl-phosphonium cation instead of a borenium cation.[34]

In our recent study, we reported the synthesis of phosphinoborenium cations and initiated reactivity investigations.[35] These species exhibit an intriguing electronic structure due to the presence of a trivalent boron Lewis acidic center bonded directly to a trivalent Lewis basic phosphorus center. Considering the ambiphilic properties of phosphinoborenium cations, we assume that these species will activate strong covalent bonds. To verify this hypothesis, we performed reactions of a specially designed phosphinoborenium cation with small molecules such as carbon dioxide, nitrous oxide, phosphine oxides, and alcohols.

Results and discussion

The starting phosphinoborenium cation **1**$^+$ was synthesized according to a method previously reported by us,[35] via the reaction of di-*tert*-butylphosphino(bromo)borane with an NHC in petroleum ether. The desired borenium salt **1[Br]** precipitated from the reaction solution and was isolated using filtration as an analytically pure white powder in a high yield (87%) (Scheme 1).

As the carbene ligand, we chose 1,3,4,5-tetramethylimidazolin-2-ylidene (IMe_4),[36] which is less prone to undesired side reactions compared with NHCs with C-H bonds in an unsaturated five-membered ring, previously used by us for the synthesis of phosphinoborenium cations. Moreover, IMe_4 has a relatively small steric hindrance, allowing small molecules to access the Lewis acidic boron center. The *i*Pr_2N amido group provides additional electronic stabilization by π-donation to the formally empty, unhybridized *p* orbital of boron. Furthermore, **1**$^+$ has Lewis basic properties due to the presence of the *t*Bu_2P phosphido moiety bonded directly to boron, where the phosphorus atom possesses an accessible lone electron pair.

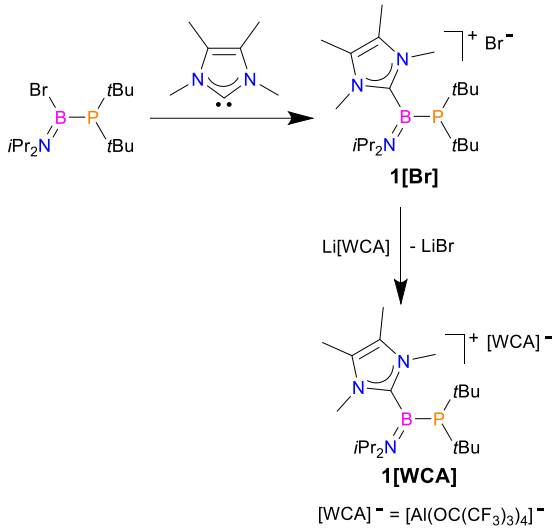

Scheme 1. Syntheses of phosphinoborenium salts **1[Br]** and **1[WCA]**.

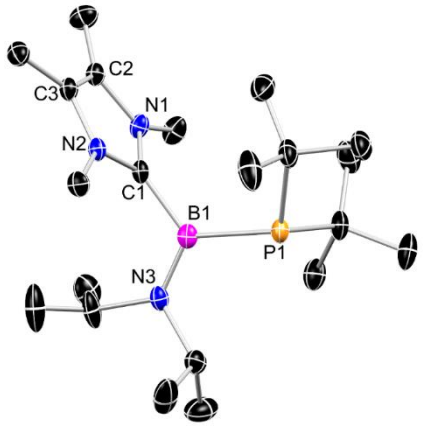

Figure 1. X-ray structure of **1[WCA]**. H-atoms and $[Al(OC(CF_3)_3)_4]^-$ counterion are omitted for clarity. The thermal ellipsoids are shown at a 30% probability level.

The spectroscopic signatures of **1**$^+$, such as the ^{11}B NMR broad resonance at 40.0 ppm and the $^{31}P\{^1H\}$ NMR broad resonance at 5.2 ppm, indicate the formation of a borenium ion with a B-P functionality. The salt **1[Br]** tends not to form crystals; however, exchanging the bromide counterion for a weakly coordinating anion ($[WCA]^- = [Al(OC(CF_3)_3)_4]^-$) followed by crystallization from dichloromethane produces crystals of **1[WCA]** (Scheme 1). Additionally, the single-crystal X-ray diffraction analysis confirmed the formation of the desired cation **1**$^+$ (Figure 1).

Having a suitable phosphinoborenium cation in hand, we tested its reactivity toward small molecules. The reactivity studies were conducted under very mild conditions, such as room temperature and atmospheric pressure, without the addition of any catalysts or external Lewis acids/bases. **1[Br]** reacted smoothly with gaseous CO_2 in dichloromethane or 1,2-difluorobenzene, resulting in the quantitative formation of **2[Br]** (Scheme 2).

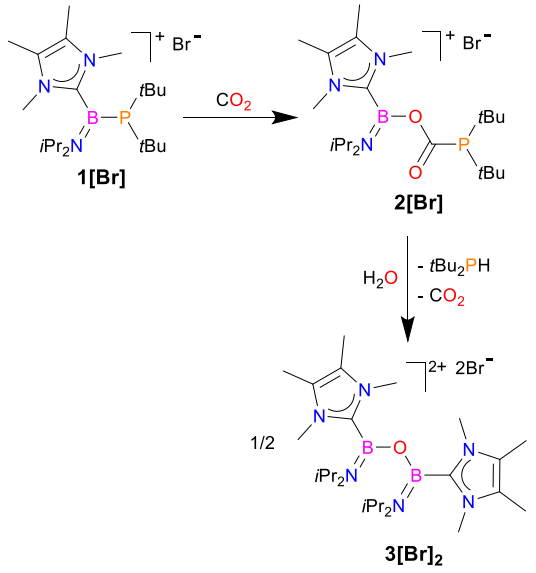

Scheme 2. Reaction of **1[Br]** with carbon dioxide and hydrolysis of phosphinoborylation product.

Progress monitoring of the reaction by ^{31}P and ^{11}B NMR spectroscopy shows the complete conversion of $\mathbf{1}^+$ into $\mathbf{2}^+$ after three hours. The borenium salt **2[Br]** was isolated as a beige powder with a 90% yield from the reaction mixture by evaporating the solvent. The product is soluble only in donor solvents such as dichloromethane or 1,2-difluorobenzene, indicating its ionic character. Compared with the parent phosphinoborenium cation $\mathbf{1}^+$, the borenium cation $\mathbf{2}^+$ displays a significantly downfield-shifted $^{31}P\{^1H\}$ sharp signal at 51.6 ppm (in comparison with 5.2 ppm of $\mathbf{1}^+$) and an upfield-shifted ^{11}B resonance at 25.3 ppm (in comparison with 40.9 ppm of $\mathbf{1}^+$), in a typical range for trivalent boron compounds. Interestingly, these chemical shifts are similar to those observed for CO_2 adducts with neutral phosphinoboranes[37,38] and diphosphinoboranes.[39] For example, tBu$_2$P-C(=O)-O-B(NiPr$_2$)$_2$ displays $^{31}P\{^1H\}$ and ^{11}B resonances at 52.4 ppm and 27.4 ppm, respectively.[38] Moreover, the $^{13}C\{^1H\}$ spectrum of **2** contains a characteristic doublet at 180.5 ppm ($^1J_{CP}$=41.7 Hz), suggesting the presence of a direct bond between the phosphorus and the carbon atom of the carbonyl group. Furthermore, integrating the signals in the ^1H NMR spectra revealed that cation $\mathbf{2}^+$ consists of one NHC ligand, two *tert*-butyl groups, and two isopropyl groups. These data suggest the insertion of CO_2 molecules into the B-P bond of the parent cation $\mathbf{1}^+$. Based on our previous studies on the reactivity of B-P bond systems, we assume that the first step in the reaction of $\mathbf{1}^+$ with CO_2 is the formation of a coordination bond between the nucleophilic P atom of $\mathbf{1}^+$ and the electrophilic carbon atom of the CO_2 molecule. Next, the oxygen atom in CO_2 attacks the electrophilic B atom, forming a new B-O bond with subsequent cleavage of the B-P bond. To our knowledge, this is the first example of CO_2 activation by a borenium cation.

Unfortunately, multiple attempts to obtain **2[Br]** crystals suitable for X-ray analysis were unsuccessful. Instead, we isolated small amounts of colorless crystals of the diborenium salt $\mathbf{3[Br]_2}$ from the crystallization solution. Its structure was determined using a single-crystal X-ray diffraction (Figure 2).

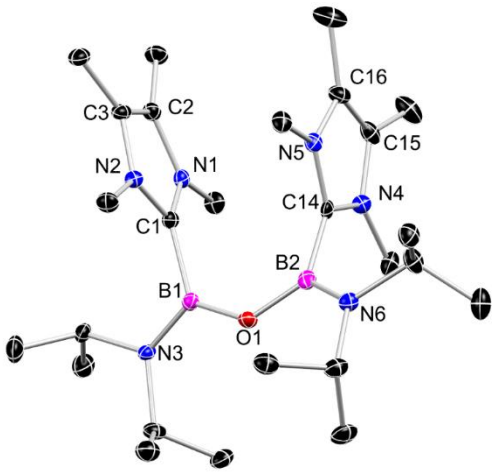

Figure 2. X-ray structure of $\mathbf{3[Br]_2}$. H-atoms, Br^- counterions, and solvent molecules (CH_2Cl_2) are omitted for clarity. The thermal ellipsoids are shown at a 30% probability level.

We assumed that dication $\mathbf{3}^{2+}$ was formed in the reaction of $\mathbf{2}^+$ with traces of water (Scheme 2). To confirm this hypothesis, we performed controlled hydrolysis of $\mathbf{2}^+$. An NMR tube was charged with a CD_2Cl_2 solution of **2[Br]** and sealed with a plastic cap. The NMR tube was left in ambient air, allowing moisture and oxygen to diffuse into the tube slowly. The hydrolysis progress was monitored using heteronuclear NMR spectroscopy (Figures S26-S32). The $^{31}P\{^1H\}$, ^{11}B, ^1H, and $^{13}C\{^1H\}$ NMR spectra recorded after 24 hours showed signal sets attributable to unreacted **2[Br]**, $\mathbf{3[Br]_2}$, and tBu$_2$PH, along with relatively weak resonances of the imidazolium salt [IMe$_4$H][Br] Based on the integration of the ^1H spectrum, the molar ratio of **2[Br]**:$\mathbf{3[Br]_2}$:tBu$_2$PH was calculated as 1:0.5:1, which is consistent with the proposed stoichiometry of the hydrolysis reaction (Scheme 2).

The NMR spectra recorded after one week showed complete hydrolysis of both **2[Br]** and $\mathbf{3[Br]_2}$ with the formation of an imidazolium salt, tBu$_2$PH and its oxide, iPr$_2$NH, and derivatives of boric acid (Figures S33-S35).

It is worth mentioning that diboreniums are a rare group of boron cations.[40–43] To our knowledge, $\mathbf{3}^{2+}$ is the first diborenium dication where the boron centers are separated by only one atom (in this case, an oxygen atom) (Figure 2).

The Stephan group reported utilizing the borenium salt [(NHC(9-BBN)][B(C$_6$F$_5$)$_4$] (NHC = 1,3-di-isopropylimidazolin-2-ylidene; 9-BBN = 9-borabicyclo(3.3.1)nonane) as the Lewis acid component of a frustrated Lewis pair in combination with tBu$_3$P to activate dihydrogen.[16] Therefore, we wanted to assess whether cation $\mathbf{1}^+$ would also activate this molecule. Unfortunately, $\mathbf{1}^+$ does not react with dihydrogen at room temperature and atmospheric pressure. The lack of reactivity of $\mathbf{1}^+$ toward H_2 can be explained by the reduced Lewis acidity of the boron center in $\mathbf{1}^+$ due to strong π-donation from the nitrogen atom of the amido group.

Subsequently, we tested the reactivity of **1**$^+$ toward nitrous oxide. The reaction of **1[Br]** with N_2O in 1,2-difluorobenzene led to the formation of **4[Br]** as a result of the insertion of an oxygen atom into the B-P bond of the parent cation and the elimination of the N_2 molecule (Scheme 3). The $^{31}P\{^1H\}$ NMR spectrum of **4**$^+$ displays a downfield-shifted sharp singlet at 163.7 ppm, in the expected range for the R_2PO phosphinite moiety. Similarly to **2**$^+$, the ^{11}B NMR resonance of **4**$^+$ is about 25 ppm. The reaction of **1**$^+$ with N_2O is much slower than the reaction with CO_2 described above. However, it can be accelerated by gentle heating of the reaction solution (50 °C), where 70% conversion of **1**$^+$ into **4**$^+$ was achieved after 7 days. Evaporating the solvent and crystallization from dichloromethane at −22 °C produced colorless crystals of **4[Br]**. The X-ray analysis of these crystals unambiguously confirmed the formation of an unprecedented borenium cation with a B-O-P functionality (Figure 3).

While exploring alternative methods of synthesizing boreniums with the R_2PO ligand, we turned our attention to secondary phosphine oxides as potential synthons. To our delight, tBu$_2$P(O)H reacted with **1[Br]** in dichloromethane, forming **4[Br]** and tBu$_2$PH (Scheme 4). The analysis of the NMR spectra of the reaction mixture indicated the complete conversion of **1**$^+$ into **4**$^+$ after 7 days. The **4[Br]** compound was isolated by evaporating the solvent and phosphine under a high vacuum, yielding a beige powder in high yield (96%).

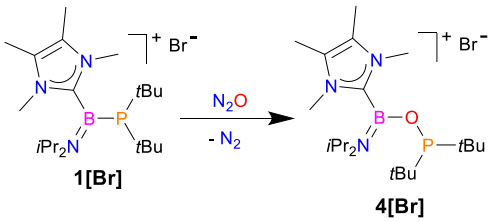

Scheme 3. Reaction of **1[Br]** with nitrous oxide.

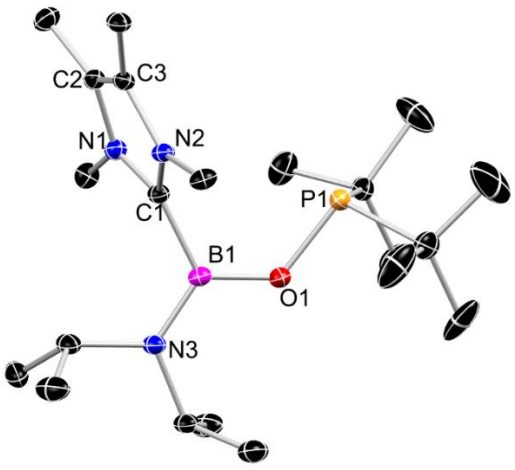

Figure 3. X-ray structure of **4[Br]**. H-atoms, Br^- counterion, and solvent molecules (1,2-difluorobenzene) are omitted for clarity. The thermal ellipsoids are shown at a 30% probability level.

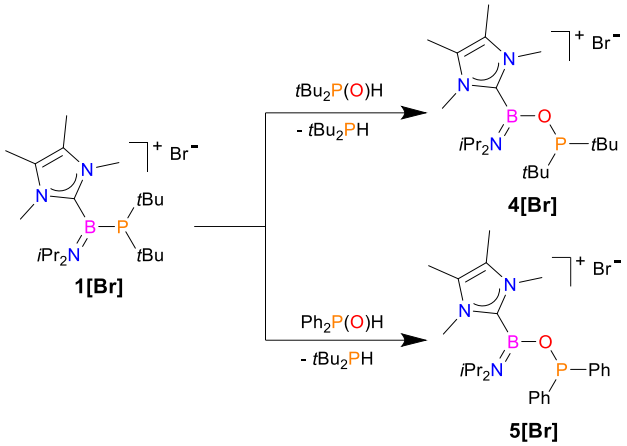

Scheme 4. Reaction of **1[Br]** with selected secondary phosphine oxides.

The question arose whether the phosphine oxide provides only the oxygen atom or the entire R_2PO fragment. To answer this question, we performed a control NMR experiment using $Ph_2P(O)H$ (Scheme 4). Similarly to the experiment involving tBu$_2$P(O)H, the reaction of **1[Br]** with $Ph_2P(O)H$ produced tBu$_2$PH as one of the main products and only one compound with a P-H functionality. Moreover, the $^{31}P\{^1H\}$ and ^{11}B NMR spectra of the reaction mixture showed resonances at 112.3 ppm and 25.4 ppm, respectively, attributable to the borenium cation **5[Br]** bearing the Ph_2PO ligand. The analysis of the $^{31}P\{^1H\}$ spectrum showed the formation of other side products, particularly the unsymmetrical diphosphane tBu$_2$PPPh$_2$.[44] The formation of the diphosphorus side product could be explained by the reaction of the starting **1[Br]** with **5[Br]**, leading to tBu$_2$P-PPh$_2$ and the diborenium cation **3[Br]$_2$**. Interestingly, in the reaction using tBu$_2$P(O)H, the formation of the diphosphane was not observed, probably due to the greater steric hindrance of the tBu$_2$P group compared with the Ph_2P fragment.

Based on the results of the experiments described above, we propose a plausible reaction pathway for the activation of secondary phosphine oxides by **1**$^+$. We hypothesize that the first step is the formation of an adduct between $R_2P(O)H$ and **1**$^+$ (B-O bond formation). In the next step, a proton is transferred from the $R_2P(H)$-O-B fragment to the Lewis basic phosphorus atom of the phosphido ligand. Subsequently, cleavage of the B-P bond allows the elimination of the R_2PH molecule.

We were curious whether phosphinoborenium cations could also be used to obtain boron cations with B-O-C functionalities. To test this, we conducted the reaction of **1[WCA]** with $(F_3C)_3COH$ in dichloromethane (Scheme 5). This reaction proceeded cleanly, yielding only two products: borenium salt **6[WCA]** and tBu$_2$PH. According to the NMR analysis of the reaction mixture, the parent **1**$^+$ is completely consumed after 24 hours. The crude **6[WCA]** can be easily isolated by evaporating the solvent and volatile phosphine under a vacuum. Crystallization of the crude product from dichloromethane produced two crops of crystals at 4 °C and −22 °C, respectively, with an overall 54% yield.

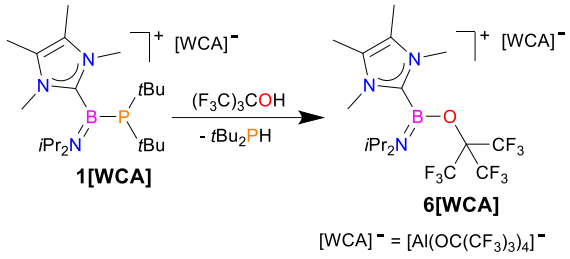

Scheme 5. Reaction of **1[WCA]** with $(F_3C)_3COH$.

6[WCA] displays a broad resonance in the ^{11}B NMR spectrum at 23.7 ppm, whereas the $^{19}F\{^1H\}$ spectrum of **6[WCA]** consists of two singlets at −72 ppm and −75.8 ppm, attributable to the CF_3 groups of **6**$^+$ and $[WCA]^-$, respectively. The X-ray analysis of isolated crystals of **6[WCA]** confirmed the attachment of the $OC(CF_3)_3$ ligand to the borenium center (Figure 4).

Encouraged by the successful synthesis and isolation of **6[WCA]**, we decided to utilize **1**$^+$ as a synthon for rare and intriguing diborenium dications. For this purpose, we reacted two equivalents of **1[WCA]** with one equivalent of tetrafluorohydroquinone in dichloromethane (Scheme 6). After 1 hour, the $^{31}P\{^1H\}$ and ^{11}B NMR resonances of **1**$^+$ disappeared. Instead, signals of tBu$_2$PH in the ^{31}P NMR spectrum and a broad singlet of the diborenium cation **7**$^{2+}$ at about 25 ppm in the ^{11}B NMR spectrum were observed. According to the analysis of the ^1H, $^{13}C\{^1H\}$, and ^{11}B spectra of **7**$^{2+}$, both (NHC)BNiPr$_2$ fragments are chemically equivalent. **7[WCA]$_2$** was isolated as a white powder in a manner analogous to **6[WCA]**, with a yield of 93%. The X-ray analysis of colorless crystals of **7[WCA]$_2$** shows that the OC_6F_4O unit acts as a linker binding two borenium centers via two B-O bonds (Figure 5).

We propose that the reaction of **1**$^+$ with alcohols proceeds via the protonation of the phosphido ligand of the borenium cation by the alcohol molecule, followed by nucleophilic attack of the alkoxide anion on the borenium center, forming a new B-O bond. In the final step, the B-P bond is cleaved, and the tBu$_2$PH molecule leaves the coordination sphere of boron.

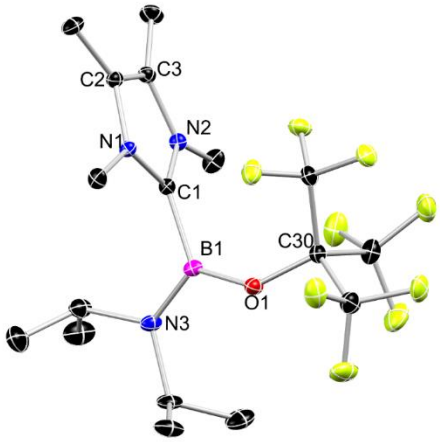

Figure 4. X-ray structure of **6[WCA]**. H-atoms and $[Al(OC(CF_3)_3)_4]^-$ counterion are omitted for clarity. The thermal ellipsoids are shown at a 30% probability level.

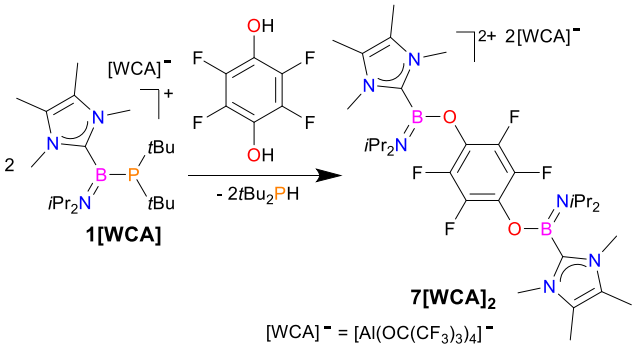

Scheme 6. Reaction of **1[WCA]** with tetrafluorohydroquinone.

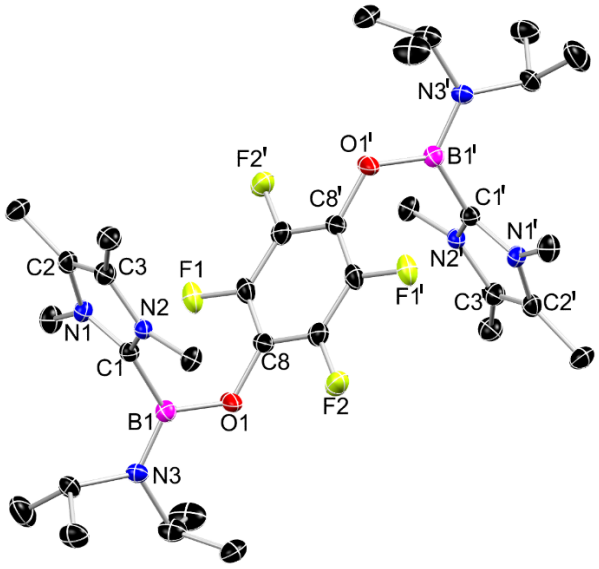

Figure 5. X-ray structure of **7[WCA]$_2$**. H-atoms and $[Al(OC(CF_3)_3)_4]^-$ counterions and solvent molecules (CH_2Cl_2) are omitted for clarity. The thermal ellipsoids are shown at a 30% probability level.

The isolation of **1[WCA]**, **3[Br]$_2$**, **4[Br]**, **6[WCA]**, and **7[WCA]$_2$** in crystalline form allows us to discuss their solid-state structures in detail. These species are borenium salts; therefore, the respective cations possess many common structural features. The central B1 atom is coordinated by the C1 atom of the NHC ligand, the N3/N6 atom of the amido group, and the P1 atom or O1 atom of other ligands. These atoms all lie in the same plane, indicating planar trigonal geometry around the central B1 atom. The torsion angle between the mentioned plane and the NHC ring varies from 73.88° to 83.21°. The planar geometry of the amido ligand indicates strong π-donation from N3/N6 atoms to the electrophilic B1 atom. In the case of **1**$^+$ and **4**$^+$, the geometry around the P1 atom is pyramidal, confirming the presence of a lone electron pair at the phosphorus atoms. The B1-C1 bond distances are about 1.6 Å, which is typical for NHC-stabilized borenium cations.[6] The B-N bond distances range from 1.373(9) Å to 1.393(4) Å, which is close to the sum of the double covalent bond radii of B and N (1.38 Å).[45] For the activation products **3[Br]$_2$**, **4[Br]**, **6[WCA]**, and **7[WCA]$_2$**, the B-O bond lengths vary from 1.376(4) Å to 1.394(9) Å and are between the expected bond distances for single and double covalent bonds (B-O: 1.48

Å; B=O: 1.35 Å).[45,46] Moreover, these borenium salts exhibit the bond angles B-O-X (X = B, P, C) within a range of 124.5(5)° to 137.2(2)°.

Furthermore, the electronic structure of parent **1**$^{+}$ and activation products **2**$^{+}$, **3**$^{2+}$, **4**$^{+}$, **6**$^{+}$, and **7**$^{2+}$ were investigated using DFT methods. The borenium character of all cations was confirmed using natural population analysis (NPA), where the largest positive charge was found for the boron atoms. A comparison of the NPA charges localized on boron (+0.662 a.u.) in **1**$^{+}$, and activation products (**2**$^{+}$, **3**$^{2+}$, **4**$^{+}$, **6**$^{+}$, and **7**$^{2+}$) indicates an increase (of approximately +0.4 a.u.) in the positive charge on B atoms upon forming the B-O-C, B-O-B, and B-O-P structural motifs in the activation products. This reduction in the electron density at the borenium center in activation products is clearly related to the fact that the oxygen atom is more electronegative than phosphorus (which is bonded directly to the boron atom in parent cation **1**$^{+}$). Natural bond orbital analysis (NBO) revealed strong π-donation from the N atoms of the amido groups to the Lewis acidic boron center, resulting in the double bond character of the B=N bonds. Using the second-order perturbation analysis, we found additional stabilizing π-interactions between the unhybridized *p* orbital of oxygen atoms and antibonding π*(B-N) orbitals. Interestingly, in the case of diborenium cation **3**$^{2+}$, both boron centers are involved in these interactions. The calculated energies of such donor-acceptor interactions are in the range of 32.01 – 50.28 kcal/mol. The thermodynamics for the reactions of **1**$^{+}$ with small molecules (as presented on Schemes 2–6) were verified by calculating the Gibbs free energy (**ΔG**^{298}) at T=298 K (Table 1). The negative **ΔG**^{298} values for all considered reactions confirmed that all processes are spontaneous at room temperature. According to our calculations, the most exergonic reaction is the activation of N_2O (**ΔG**^{298} = –106.4 kcal/mol), while CO_2 activation is characterized by the smallest release of free energy (**ΔG**^{298} = –7.7 kcal/mol).

Table 1. Gibbs free energies (ΔG^{298} in kcal/mol) predicted for the reaction phosphinoborenium cation **1**$^{+}$ with small molecules determined at the ωB97xD/6-311++G(d,p) level and in dichloromethane solution.

Reaction path	**ΔG**^{298} (kcal/mol)
1^{+}+ CO_2 → **2**$^{+}$	–7.7
2×**2**$^{+}$ + H_2O → **3**$^{2+}$ + 2×*t*Bu_2PH + 2×CO_2	–46.6
1^{+} + N_2O → **4**$^{+}$ + N_2	–106.4
1^{+} + *t*Bu_2P(O)H → **4**$^{+}$ + *t*Bu_2PH	–26.6
1^{+} + $(F_3C)_3COH$ → **6**$^{+}$ + *t*Bu_2PH	–27.7
2×**1**$^{+}$ + $C_6F_4(OH)_2$ → **7**$^{2+}$ + 2×*t*Bu_2PH	–63.4

Conclusions

We confirmed the ambiphilic properties of the phosphinoborenium cation in reactions involving CO_2, N_2O, secondary phosphine oxides, and alcohols. The title compound mimics the reactivity of intramolecular frustrated Lewis pairs, where Lewis basic and Lewis acidic centers interact cooperatively with a substrate. Two reactivity patterns can be distinguished among the reactions of **1**$^{+}$ with small molecules. Aprotic molecules such as CO_2 or N_2O react with **1**$^{+}$ by inserting the whole molecule or its fragment into the B-P bond of the parent cation. In contrast, reactions of **1**$^{+}$ with protic molecules such as secondary phosphine oxides and alcohols proceed via protonation of the *t*Bu_2P phosphido ligand of **1**$^{+}$, formation of a new B-O bond, and subsequent cleavage of the B-P bond, leading to the elimination of the *t*Bu_2PH molecule. As a result of these reactions, a series of unprecedented borenium and diborenium cations with B-O-C(=O)-P, B-O-P, and B-O-C structural motifs were obtained. The next stage of our research will be the application of ambiphilic B-P cations in catalytic transformations.

Conflicts of interest

There are no conflicts to declare

Acknowledgements

Financial support of these studies from Gdańsk University of Technology by the DEC-20/2021/IDUB/I.3.3 grant under the ARGENTUM and by the DEC-2/2021/IDUB/V.6/Si grant under the SILICIUM - 'Excellence Initiative - Research University' program is gratefully acknowledged.

Notes and references

1 T. S. De Vries, A. Prokofjevs and E. Vedejs, *Chem Rev*, 2012, **112**, 4246–4282.

2 W. E. Piers, S. C. Bourke and K. D. Conroy, *Angewandte Chemie - International Edition*, 2005, **44**, 5016–5036.

3 P. Kolle and H. Nöth, *Chem Rev*, 1985, **85**, 399–418.

4 V. Nesterov, D. Reiter, P. Bag, P. Frisch, R. Holzner, A. Porzelt and S. Inoue, *Chem Rev*, 2018, **118**, 9678–9842.

5 A. Doddi, M. Peters and M. Tamm, *Chem Rev*, 2019, **119**, 6994–7112.

6 T. Matsumoto and F. P. Gabbai, *Organometallics*, 2009, **28**, 4252–4253.

7 D. McArthur, C. P. Butts and D. M. Lindsay, *Chemical Communications*, 2011, **47**, 6650–6652.

8 A. Solovyev, S. J. Geib, E. Lacôte and D. P. Curran, *Organometallics*, 2012, **31**, 54–56.

9 H. B. Mansaray, A. D. L. Rowe, N. Phillips, J. Niemeyer, M. Kelly, D. A. Addy, J. I. Bates and S. Aldridge, *Chemical Communications*, 2011, **47**, 12295–12297.

10 J. M. Farrell, D. Schmidt, V. Grande and F. Würthner, *Angewandte Chemie - International Edition*, 2017, **56**, 11846–11850.

11 J. M. Farrell and D. W. Stephan, *Angewandte Chemie - International Edition*, 2015, **54**, 5214–5217.

12 J. M. Farrell, R. T. Posaratnanathan and D. W. Stephan, *Chem Sci*, 2015, **6**, 2010–2015.

13 A. Prokofjevs, J. W. Kampf, A. Solovyev, D. P. Curran and E. Vedejs, *J Am Chem Soc*, 2013, **135**, 15686–15689.

14 Y. Wang and G. H. Robinson, *Inorg Chem*, 2011, **50**, 12326–12327.

15 P. Eisenberger and C. M. Crudden, *Dalton Transactions*, 2017, **46**, 4874–4887.

16 J. M. Farrell, J. A. Hatnean and D. W. Stephan, *J Am Chem Soc*, 2012, **134**, 15728–15731.

17 P. Eisenberger, B. P. Bestvater, E. C. Keske and C. M. Crudden, *Angewandte Chemie - International Edition*, 2015, **54**, 2467–2471.

18 B. S. N. Huchenski, M. R. Adams, R. McDonald, M. J. Ferguson and A. W. H. Speed, *Organometallics*, 2016, **35**, 3101–3104.

19 J. Lam, B. A. R. Günther, J. M. Farrell, P. Eisenberger, B. P. Bestvater, P. D. Newman, R. L. Melen, C. M. Crudden and D. W. Stephan, *Dalton Transactions*, 2016, **45**, 15303–15316.

20 D. M. Mercea, M. G. Howlett, A. D. Piascik, D. J. Scott, A. Steven, A. E. Ashley and M. J. Fuchter, *Chemical Communications*, 2019, **55**, 7077–7080.

21 A. Prokofjevs, A. Boussonnière, L. Li, H. Bonin, E. Lacôte, D. P. Curran and E. Vedejs, *J Am Chem Soc*, 2012, **134**, 12281–12288.

22 X. Pan, A. Boussonnière and D. P. Curran, *J Am Chem Soc*, 2013, **135**, 14433–14437.

23 A. Boussonnière, X. Pan, S. J. Geib and D. P. Curran, *Organometallics*, 2013, **32**, 7445–7450.

24 J. E. Radcliffe, V. Fasano, R. W. Adams, P. You and M. J. Ingleson, *Chem Sci*, 2019, **10**, 1434–1441.

25 J. S. McGough, S. M. Butler, I. A. Cade and M. J. Ingleson, *Chem Sci*, 2016, **7**, 3384–3389.

26 J. R. Lawson, E. R. Clark, I. A. Cade, S. A. Solomon and M. J. Ingleson, *Angewandte Chemie - International Edition*, 2013, **52**, 7518–7522.

27 A. Prokofjevs, J. W. Kampf and E. Vedejs, *Angewandte Chemie - International Edition*, 2011, **50**, 2098–2101.

28 V. Bagutski, A. Del Grosso, J. A. Carrillo, I. A. Cade, M. D. Helm, J. R. Lawson, P. J. Singleton, S. A. Solomon, T. Marcelli and M. J. Ingleson, *J Am Chem Soc*, 2013, **135**, 474–487.

29 T. S. De Vries, A. Prokofjevs, J. N. Harvey and E. Vedejs, *J Am Chem Soc*, 2009, **131**, 14679–14687.

30 B. Su, Y. Li, Z. H. Li, J.-L. Hou and H. Wang, *Organometallics*, 2020, **39**, 4159–4163.

31 M. Devillard, R. Brousses, K. Miqueu, G. Bouhadir and D. Bourissou, *Angewandte Chemie - International Edition*, 2015, **54**, 5722–5726.

32 M. Devillard, S. Mallet-Ladeira, G. Bouhadir and D. Bourissou, *Chemical Communications*, 2016, **52**, 8877–8880.

33 W. Lv, Y. Dai, R. Guo, Y. Su, D. A. Ruiz, L. L. Liu, C. Tung and L. Kong, *Angewandte Chemie*, 2023, **135**, e202308467.

34 M. A. Dureen, A. Lough, T. M. Gilbert and D. W. Stephan, *Chemical Communications*, 2008, **913**, 4303–4305.

35 K. Kaniewska-Laskowska, A. Ordyszewska, T. Wojnowski, H. Halenka, M. Czapla, J. Chojnacki and R. Grubba, *Dalton Transactions*, 2023, **52**, 16061–16066.

36 N. Kuhn and T. Kratz, *Synthesis (Stuttg)*, 1993, **1993**, 561–562.

37 J. H. W. LaFortune, Z. W. Qu, K. L. Bamford, A. Trofimova, S. A. Westcott and D. W. Stephan, *Chemistry - A European Journal*, 2019, **25**, 12063–12067.

38 N. Szynkiewicz, A. Ordyszewska, J. Chojnacki and R. Grubba, *RSC Adv*, 2019, **9**, 27749–27753.

39 N. Szynkiewicz, A. Ordyszewska, J. Chojnacki and R. Grubba, *Inorg Chem*, 2021, **60**, 3794–3806.

40 Y. Dai, Z. Xie, M. Bao, C. Liu and Y. Su, *Chem Sci*, 2023, **14**, 3548–3553.

41 D. Franz, T. Szilvási, A. Pöthig, F. Deiser and S. Inoue, *Chemistry – A European Journal*, 2018, **24**, 4283–4288.

42 A. Widera, E. Filbeck and H. Himmel, *Eur J Inorg Chem*, 2020, **2020**, 3017–3029.

43 D. Parveen, R. K. Yadav, B. Mondal, M. Dallon, Y. Sarazin and D. K. Roy, *Dalton Transactions*, , DOI:10.1039/d4dt02050b.

44 N. Szynkiewicz, Ł. Ponikiewski and R. Grubba, *Dalton Transactions*, 2018, **47**, 16885–16894.

45 P. Pyykkö and M. Atsumi, *Chemistry - A European Journal*, 2009, **15**, 12770–12779.

46 P. Pyykkö and M. Atsumi, *Chemistry - A European Journal*, 2009, **15**, 186–197.